INTERNATIONAL JOURNAL OF NUMERICAL MODELLING: ELECTRONIC NETWORKS, DEVICES AND FIELDS
Int. J. Numer. Model. 2006; **19**:301–314
Published online 11 May 2006 in Wiley InterScience (www.interscience.wiley.com). DOI: 10.1002/jnm.613

FETMOSS: a software tool for 2D simulation of double-gate MOSFET

Tarek M. Abdolkader[1,*,†], Wael Fikry Farouk[2], O. A. Omar[3] and Mahmoud Fathy Mahmoud Hassan[1]

[1] *Department of Basic Sciences, Benha Higher Institute of Technology, Egypt*
[2] *Mentor Graphics Egypt, Egypt*
[3] *Department of Engineering Physics and Mathematics, Faculty of Engineering, Ain Shams University, Egypt*

SUMMARY

A software tool for the 2D simulation of double-gate SOI MOSFET is developed. The developed tool is working under MATLAB environment and is based on the numerical solution of Poisson and Schrödinger equations self-consistently to yield the potential, carrier concentrations, and current within the device. Compared to the already existing tools, the new tool uses finite elements method for the solution of Poisson equation, thus, the simulation of curved boundary structures becomes feasible. Another new feature of the tool is the use of transfer matrix method (TMM) in the solution of Schrödinger equation which was proven in a recent published paper that it gives more accurate results than the conventional finite difference method (FDM) when used in some regions of operation. According to the working conditions, the tool can toggle between FDM and TMM to satisfy the highest accuracy with the largest speed of simulation. The tool is named as FETMOSS (Finite Elements and Transfer matrix MOS Simulator). Copyright © 2006 John Wiley & Sons, Ltd.

Received 1 September 2005; Revised 1 February 2006; Accepted 12 March 2006

KEY WORDS: device simulation; double-gate MOSFET; quantum-mechanical effects; FETMOSS

1. INTRODUCTION

For the design of semiconductor devices, it is required to (1) explain physical phenomena occurring in the device, (2) predict the device response to possible variations. Three main methodologies are used to satisfy these objectives: experimental measurements, analytical modelling, and computer-aided design (CAD) tools. In recent years, the use of CAD tools has received broad acceptance among the silicon technology community owing to its superior capabilities in comparison to the other two alternatives. Experimental measurements suffer from

*Correspondence to: T. M. Abdolkader, Department of Basic Sciences, Benha Higher Institute of Technology, Egypt.
† E-mail: tarik_mak@hotmail.com

excessive costs and infeasibility in some cases. On the other hand, with the ever-increasing miniaturization of semiconductor devices through very large-scale integration (VLSI), the complexity of the device physics with pronounced quantum-mechanical effects disables the use of analytical modelling. Software tools based on the numerical simulation of device operation (device simulators) enable the designer to easily perform parametric studies to explore the effect of various parameters on the device operation far from excessive costs of experimental investigation. Moreover, only with device simulators it is possible to accurately predict the device performance prior fabrication, thus, the number of fabrication trials and errors are substantially reduced and the design cost and time are much decreased. It is concluded that the use of device simulators is indispensable alternative for efficient device design.

Several classical device simulators were developed for the simulation of conventional MOSFETs [1–4], but a few which take care of quantum effects in nanoscale devices have been found [5, 6]. In this work, a two dimensional (2D) quantum-mechanical device simulation tool for nanoscale double-gate (DG) SOI MOSFETs was developed. The tool is working under MATLAB environment and is based on the self-consistent numerical solution of Poisson and Schrödinger equations. The Poisson equation is solved by finite elements method (FEM) [7] using the partial differential equations (PDE) toolbox of MATLAB. On the other hand, Schrödinger equation is solved using mode-space representation [8] which much reduces the computational burden. The discretization of Schrödinger equation is performed by either the finite difference method (FDM) [9] or transfer matrix method (TMM) [10]. The choice between the two methods is according to the silicon film thickness and the operating temperature aiming to compromise between the predefined accuracy and the minimum simulation time.

In Section 2, the algorithm of the main program is presented. In Section 3, it is explained how to solve Poisson equation using PDE toolbox of MATLAB. The mode-space representation along with a comparison between FDM and TMM, used for the solution of Schrödinger equation, is given in Section 4. A group of results of the program are shown and discussed in Section 5. Finally, conclusion is drawn in Section 6.

2. THE MAIN PROGRAM

Nanoscale semiconductor devices are described electrically on quantum-mechanical level by two main equations: the first is Poisson equation,

$$\nabla^2 V = -\frac{q}{\varepsilon}(p - n + N_{\mathrm{D}} - N_{\mathrm{A}}) \tag{1}$$

from which the electrical potential V can be determined given the quantities on the right-hand side including hole and electron distributions p and n, and doping concentrations for donors and acceptors N_{D} and N_{A}, respectively. In (1), q is electronic charge, and ε is the permittivity of the medium. The simulation tool developed is devoted to n-MOSFETs, where hole concentration is neglected. The second equation is Schrödinger equation with effective mass approximation,

$$\frac{-\bar{h}^2}{2m^*}\nabla^2\psi - (qV + E)\psi = 0 \tag{2}$$

which, given the electric potential V, determines eigenenergies E and eigenfunctions ψ from which the electron concentration can be obtained. In (2), $\bar{h}$ is the modified Planck's constant and m^* is the effective mass of electrons. The transport of carriers in nanoscale DG devices is nearly

DOI: 10.1002/jnm

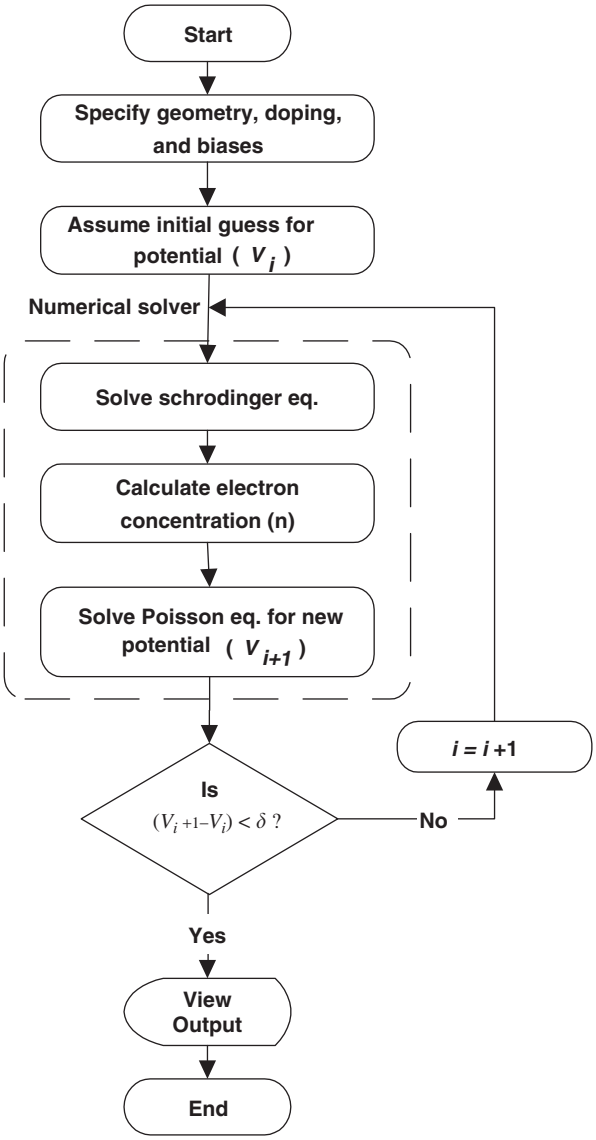

Figure 1. Flow chart of the main program FETMOSS.

ballistic [11], so, no scattering are included in the solution of (2). Equations (1) and (2) are coupled such that the solution of any one requires the result of the other; consequently, they are solved by iterative method until self-consistence is obtained.

The flow chart of the main program is shown in Figure 1. A rough initial guess for the potential distribution in the device is firstly assumed. According to this potential, Schrödinger equation is solved. The eigenenergies and eigenfunctions resulting from the solution of Schrödinger equation are used to calculate the electron concentration in the device. Now, with

DOI: 10.1002/jnm

the electron concentration is known, Poisson equation can be solved yielding a new potential distribution. The new potential is compared to the old potential and the solution cycle is repeated until self-consistent solution for the potential is obtained (until the difference in potential between two successive iterations is below a certain tolerance, δ).

3. SOLVING SCHRODINGER EQUATION

The Schrödinger is discretized using mode-space representation approach. This approach greatly reduces the size of the problem and provides sufficient accuracy when compared to full 2D spatial discretization [8]. Referring to Figure 2, a model DG SOI device is divided into vertical slices, each of width a. For each vertical slice at $x = x'$, a 1D effective mass equation in the z direction is written as

$$\frac{-\bar{h}^2}{2m_z^*}\frac{\mathrm{d}^2\psi(x',z)}{\mathrm{d}z^2} + (U(x',z) - E)\psi(x',z) = 0 \tag{3}$$

where m_z^* is the effective mass of electrons in the z direction and $U = -qV$ is the potential energy. This equation is solved subject to zero boundary conditions at both upper and lower interfaces assuming nearly infinite conduction band offset between Si and SiO_2, (nearly infinite potential barriers imposed by upper and lower oxides means zero eigenfunction there) to obtain a discrete set of eigenenergies and corresponding eigenfunctions, i.e. a set of modes. For each mode m, the distribution of eigenenergies $E_m(x)$ along the x direction resulting from the solution of (3) is used to solve the 1D Schrödinger equation in the x direction,

$$\frac{-\bar{h}^2}{2m_x^*}\frac{\mathrm{d}^2\varphi^{(m)}(x)}{\mathrm{d}x^2} - (E - E_m(x))\varphi^{(m)}(x) = 0 \tag{4}$$

subject to open boundary conditions at source (left boundary) and drain (right boundary), where m_x^* is the effective mass of electrons in the x direction. Equation (4) is solved twice, one assuming a plane wave is incident from the source contact, in which the solution is termed $\varphi_S^{(m)}$, and the other assuming a plane wave is incident from the drain contact, where the solution is

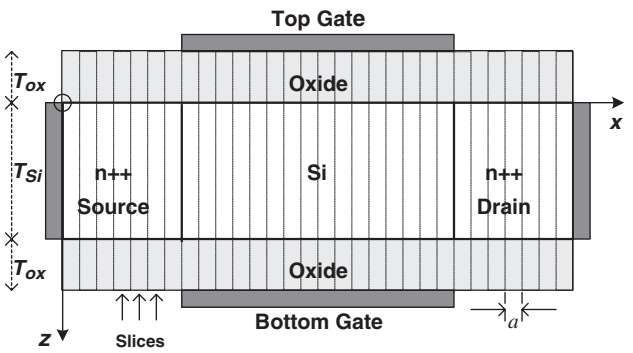

Figure 2. A model double-gate SOI device divided into vertical slices.

DOI: 10.1002/jnm

termed $\varphi_{\mathrm{D}}^{(m)}$. The m-mode contribution to the total electron density is thus found from [12],

$$n^{(m)} = \frac{1}{\hbar a}\sqrt{\frac{m_y^* k_{\mathrm{B}} T}{2\pi^3}} \int_0^\infty [\Im_{-1/2}(F_{\mathrm{S}} - E)|\varphi_{\mathrm{S}}^{(m)}(x)|^2 + \Im_{-1/2}(F_{\mathrm{D}} - E)|\varphi_{\mathrm{D}}^{(m)}(x)|^2]\,\mathrm{d}E \tag{5}$$

where $\hbar$ is the modified Planck's constant, m_y^* the effective mass of electrons in the y direction, k_{B} the Boltzmann constant, T the temperature, $\Im_{-1/2}$ the Fermi–Dirac integral of order $-1/2$ [13], and F_{S} and F_{D} are the Fermi levels at source and drain contacts, respectively.

The total electron density within the device is found by the sum of all contributions of individual modes weighted by the probability function $|\psi_m(x,z)|^2$ of each mode resulting from the solution of (3), i.e.

$$n(x,z) = \sum_m n^{(m)}|\psi_m(x,z)|^2 \tag{6}$$

From a computational point of view, If we have N_z points in the z direction and N_x points in the x direction, the full 2D discretization will lead to $N_z N_x$ points and this requires the solution of $N_z N_x \times N_z N_x$ matrices. On the other hand, using the above mode-space approach, we solve $N_z \times N_z$ matrices in the z direction to find modes, then, we solve $N_x \times N_x$ matrices in the x direction for each mode. The number of operations in mode space is on the order of $N_x \times (N_z \times N_z) + N_m \times (N_x \times N_x)$, where N_m is the number of modes. Therefore, if only the first few modes are taken into account, the latter approach provides enormous savings in the computational burden [14].

For the solution of (3) the developed program FETMOSS uses either FDM or TMM. In both methods, the domain of solution is divided into small intervals and a certain approximation, as explained hereinafter, is made within each interval such that the differential equation is transformed to a system of equations which solved to yield the eigenenergies and the distribution of the wave function. The application of the FDM and TMM for the solution of Schrödinger equation in the transverse direction of DG SOI MOSFET is explained in the following two subsections, respectively.

3.1. Finite difference method

The FDM subdivides the simulation domain into small discrete segments separated by nodal points (see Figure 3). The method is based on defining unknown variable only on these nodal points assuming linear variation in between. The derivatives in the differential equation to be solved are thus replaced by discretized finite-difference approximations at each one of the nodes. Using the notations: i for the index of node, and f_i for the value of the function to be determined at node i, one can write,

$$f'(z_i) \cong \frac{f_{i+1} - f_i}{a} = \frac{f_i - f_{i-1}}{a} \tag{7}$$

and

$$f''(z_i) \cong \frac{((f_{i+1} - f_i)/a) - ((f_i - f_{i-1})/a)}{a} = \frac{f_{i-1} - 2f_i + f_{i+1}}{a^2} \tag{8}$$

Applying Equation (8) on the 1D Schrödinger equation given in (3), we obtain

$$-\eta(\psi_{i-1} - 2\psi_i + \psi_{i+1}) + U_i\psi_i = E\psi_i \tag{9}$$

DOI: 10.1002/jnm

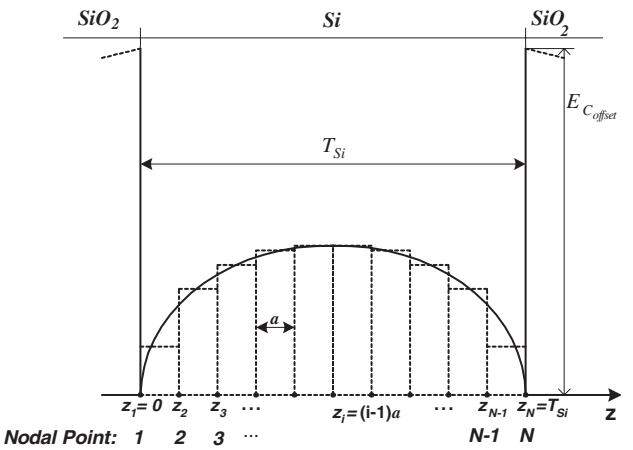

Figure 3. Conduction band edge across the transverse direction (normal to the interface) of a DG-nMOSFET. Using FDM, the domain is discretized through N nodal points equally separated by distance a.

where $\eta = \hbar^2/2m^*a^2$. Equation (9) is a compact representation of N-2 equations at N-2 interior points. The two points at the boundaries needs special treatment. At the left boundary (point 1), Equation (9) becomes,

$$-\eta(\psi_0 - 2\psi_1 + \psi_2) + U_1\psi_1 = E\psi_1 \tag{10}$$

And, at the right boundary (point N), becomes,

$$-\eta(\psi_{N-1} - 2\psi_N + \psi_{N+1}) + U_N\psi_N = E\psi_N \tag{11}$$

In (10) and (11), ψ_0 and ψ_{N+1} are the wave functions at the hypothetical points 0 and $N+1$ outside the simulation domain and should be determined from the boundary conditions. For example, in the transverse direction of DG SOI MOSFET, the domain is surrounded by infinite potential barriers of zero wave function, thus,

$$\psi_0 = \psi_{N+1} = 0 \tag{12}$$

The complete set of Equations (9)–(11) with condition (12) is cast in matrix form as

$$\begin{bmatrix} 2\eta + U_1 & -\eta & 0 & \dots & 0 \\ -\eta & 2\eta + U_2 & -\eta & \ddots & 0 \\ 0 & -\eta & \ddots & -\eta & 0 \\ \vdots & \ddots & -\eta & 2\eta + U_{N-1} & -\eta \\ 0 & \dots & 0 & -\eta & 2\eta + U_N \end{bmatrix} \begin{bmatrix} \psi_1 \\ \psi_2 \\ \vdots \\ \psi_{N-1} \\ \psi_N \end{bmatrix} = E \begin{bmatrix} \psi_1 \\ \psi_2 \\ \vdots \\ \psi_{N-1} \\ \psi_N \end{bmatrix} \tag{13}$$

This eigenvalue equation is solved for N different modes. Each mode has an eigenenergy $E^{(m)}$, and corresponding eigenfunction values, $\psi_1^{(m)}, \psi_2^{(m)}, \dots, \psi_N^{(m)}$ at the N nodal points.

DOI: 10.1002/jnm

3.2. Transfer matrix method

As mentioned previously, both FDM and TMM is based on breaking up the domain of solution into N segments, where in each segment, the potential energy is assumed constant. However, TMM is different from FDM in that the wave function within each segment is not assumed linear, but, it takes as an exponential (or sinusoidal) form as deduced from the exact solution of the wave equation in constant potential regions. Consequently, for the ith segment, the wave function can be approximated as

$$\psi_i(z) = A_i \exp(\alpha_i z) + B_i \exp(-\alpha_i z) \tag{14}$$

With

$$\alpha_i = \sqrt{2m_z^*(U_i - E)}/\hbar \tag{15}$$

Applying the conditions of continuity for $\psi(z)$ and $\mathrm{d}\psi(z)/\mathrm{d}z$ between each two successive segments, we arrive at a series of matrix equations relating A_i and B_i of any segment with those of the preceding segment A_{i-1} and B_{i-1} as follows:

$$\begin{bmatrix} A_{i-1} \\ B_{i-1} \end{bmatrix} = \mathbf{M}^{-1}(\alpha_{i-1}, z_{i-1})\mathbf{M}(\alpha_i, z_{i-1}) \begin{bmatrix} A_i \\ B_i \end{bmatrix} \tag{16}$$

with

$$\mathbf{M}(\alpha_i, z_j) = \begin{bmatrix} \mathrm{e}^{\alpha_i z_j} & \mathrm{e}^{-\alpha_i z_j} \\ \alpha_i \mathrm{e}^{\alpha_i z_j} & -\alpha_i \mathrm{e}^{-\alpha_i z_j} \end{bmatrix} \tag{17}$$

For bound states solution, A of the right boundary segment (A_R) and B for the left boundary segment (B_L) must vanish [15]. Thus, on eliminating the intermediate coefficients from (16), we obtain,

$$\begin{bmatrix} A_\mathrm{L} \\ 0 \end{bmatrix} = \mathbf{M}^{-1}(\alpha_\mathrm{L}, 0) \cdot \mathbf{\Pi} \cdot \mathbf{M}(\alpha_\mathrm{R}, z_N) \begin{bmatrix} 0 \\ B_\mathrm{R} \end{bmatrix} \tag{18}$$

where

$$\mathbf{\Pi} = \mathbf{P}_1 \mathbf{P}_2 \ldots \mathbf{P}_\mathrm{N} \tag{19}$$

And

$$\mathrm{P}_i = \mathbf{M}(\alpha_i, z_{i-1})\mathbf{M}^{-1}(\alpha_i, z_i) \tag{20}$$

Applying zero eigenfunction boundary conditions, it is found that the matrix element $\mathbf{\Pi}_{12}$ must vanish, i.e.

$$\mathbf{\Pi}_{12} = 0 \tag{21}$$

This condition represents an implicit equation that determines all the eigenenergies. In addition, for each eigenenergy, the corresponding eigenfunction is determined by calculating the coefficients A_n and B_n for each segment from (16).

It was proven in previous published paper [10] that TMM is more accurate than FDM. This superiority of TMM is more evident for higher eigenenergies than lower ones. This was explained by the rapid change of the eigenfunctions of higher energies for which the assumption of linear variation of ψ within each segment supposed by FDM is fairly poor, while exponential

DOI: 10.1002/jnm

(or sinusoidal) variation assumed by TMM is more suitable. Thus, unless only the first mode is important to be taken into account in the solution, FETMOSS uses TMM in the solution of Schrödinger equation, otherwise, it uses FDM as it is relatively easy and its accuracy does not differ much from TMM for the first mode solution [10].

4. SOLVING POISSON EQUATION

Poisson equation given in (1) is solved using the PDE toolbox of MATLAB [16] which solve elliptic equations of the form,

$$-\nabla \cdot (\alpha \nabla u) + \beta u = f \tag{22}$$

where u is the unknown variable, α, β, and f can be any predefined functions of space and of the unknown variable u. The PDE toolbox uses FEM with a Delaunay triangulation [17] of the domain of solution. The first assumption used is that hole concentration is negligible for n-MOSFETs. Moreover, for better convergence of the self-consistent loop, n is replaced by a new variable, namely, the quasi-fermi potential energy for electrons F_n defined by [14],

$$n = N_C \Im_{1/2}\left(\frac{F_n + qV}{K_B T}\right) \tag{23}$$

where N_C is normalization factor, and $\Im_{1/2}(x)$ is the Fermi–Dirac integral of order $1/2$ [13] which is an integral of an exponential function of x. The advantage of introducing this variable change is that overestimates in V will increase n through (23) which leads to the decrease of V during the solution of (1). Better convergence comes on the expense of introducing nonlinearity in the equation which is solved iteratively by Newton–Raphson method [18]. Now, Poisson equation given in (1) can be written in the form,

$$-\nabla \cdot \left(\left(\frac{\varepsilon}{\varepsilon_{Si}}\right)\nabla V\right) = q(p - n + N_D - N_A) \tag{24}$$

to be compatible with (22). Comparing (24) with (22), and applying the above assumptions, we can write,

$$\alpha = (\varepsilon/\varepsilon_{Si}), \quad \beta = 0, \quad f = q\left(-N_C \Im_{1/2}\left(\frac{F_n + qV}{K_B T}\right) + N_D - N_A\right)$$

Dirichlet boundary conditions are imposed on gate contacts, whereas at all the other boundaries, Neumann boundary conditions are used [14]. Thus, boundary conditions are,

$$\begin{aligned} V &= V_{G1} \quad \text{at the upper gate contact} \\ V &= V_{G2} \quad \text{at the lower gate contact} \\ \boldsymbol{n} \cdot \nabla V &= 0 \quad \text{otherwise} \end{aligned}$$

where $\boldsymbol{n}$ is the unit outward normal unit at the specified boundary.

DOI: 10.1002/jnm

5. RESULTS AND DISCUSSION

A model DG SOI n-MOSFET device with $n+$ source/drain donor doping of 10^{20} cm^{-3} and substrate body acceptor doping 10^{10} cm^{-3} is used. Both of the top and bottom gate contact work functions are taken to be 4.25 eV. The top and bottom insulator relative dielectric constant is assumed to be 3.9, while that of Si is 11.7. The length of the gate is 9.6 nm. All simulations are performed at room temperature ($T = 300$ K). The results drawn by FETMOSS are compared with that calculated by nanomos 2.5 [12], which is a device simulator for DG SOI n-MOSFETs developed at Purdue University. Nanomos uses FDM for the solution of both Poisson and Schrödinger equations and can solve by either of five transport models. The quantum ballistic model of nanomos is adapted for extracting results used for comparison as it matches the assumptions made in FETMOSS.

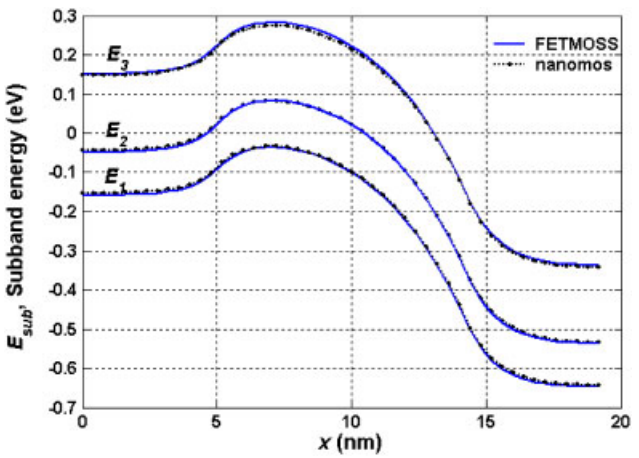

Figure 4. The distribution of the first three subband energies along the channel of the device calculated by both FETMOSS (solid lines) and nanomos (dotted lines).

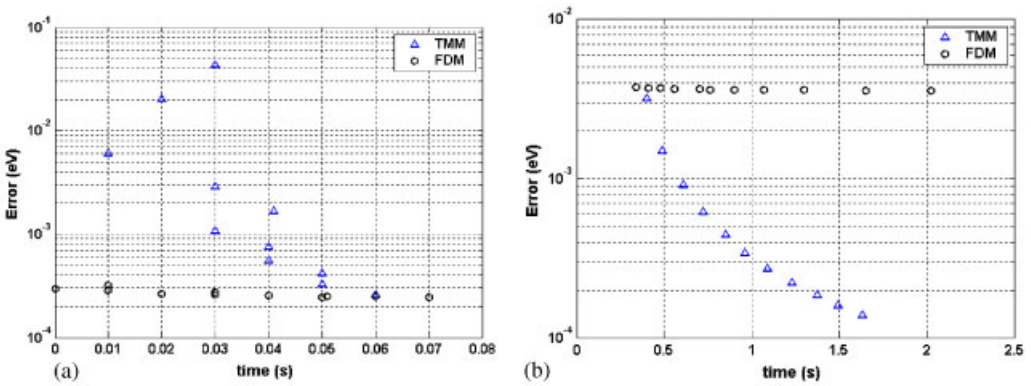

Figure 5. Comparison of the accuracy of TMM and FDM methods for:
(a) one mode, (b) five modes included.

DOI: 10.1002/jnm

In Figure 4, with the thickness of top and bottom oxides (T_{ox}) is 1.6 nm, while that of the silicon film (T_{Si}) is 3.2 nm, the distribution of eigenenergy along the channel (x direction) is shown for the first three modes with gate bias voltage $V_G = 0.25$ V and drain bias voltage $V_D = 0.5$ V. It should be noted that a discrepancy in the eigenvalues of the two methods starts to raise at the third mode. A comparison of the accuracy in the calculation of the eigenvalues for of the two methods versus time is given in Figures 5(a) and (b) for one mode and five modes included, respectively. In the latter case TMM is more accurate than FDM at the same time of simulation.

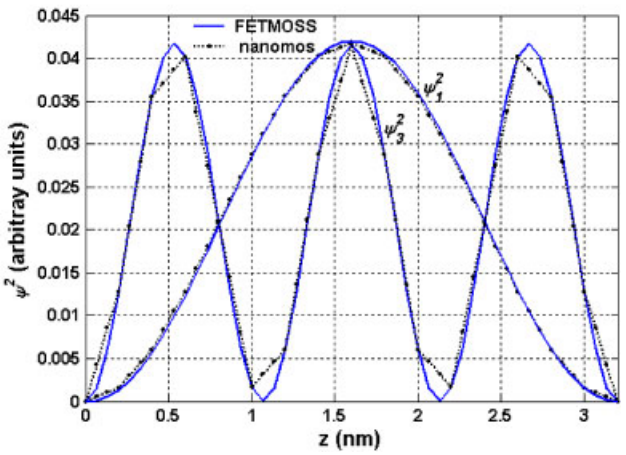

Figure 6. The distribution of the probability functions (ψ^2) of the first and third modes along z calculated at the middle of the channel ($x = T_{Si}/2$) by both nanomos 2.5 and FETMOSS simulators.

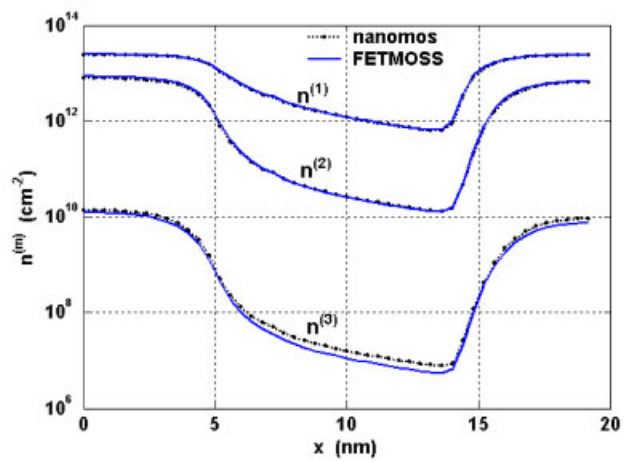

Figure 7. The 2D electron density along the channel for the first three modes. FETMOSS results are represented by the solid lines where nanomos results are represented by dotted lines.

DOI: 10.1002/jnm

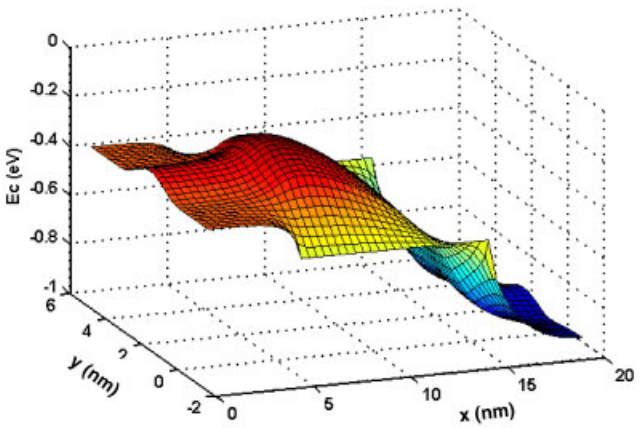

Figure 8. The 3D distribution of the conduction band edge at characteristics at $V_D = V_G = 0.7$ V.

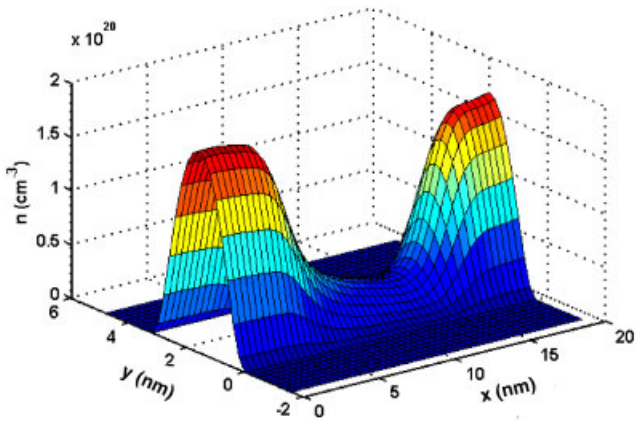

Figure 9. The 3D distribution of the electron concentration at $V_D = V_G = 0.7$ V.

On the other hand, the distribution of the probability functions (ψ^2) along z is calculated at the middle of the channel for the first and third modes by both simulators and depicted in Figure 6. It is evident from the figure that for the third mode, the use of TMM for the solution of the Schrödinger equation in FETMOSS resulted in a better smoothness in the distribution. Besides, the effect of the use of TMM can be deduced from the 2D electron density distribution along the channel as illustrated from Figure 7, where the discrepancy of results between FETMOSS and nanomos simulators is more evident for the third mode. The tool can give 3D distributions of conduction band edge and the total electron density as depicted in Figures 8 and 9, respectively.

Comparison of I_D–V_G characteristics is depicted in Figure 10 using two drain bias voltages, 0.1 and 0.6 V for a device of $T_{ox} = 1.5$ nm and $T_{Si} = 5$ nm. The results of FETMOSS and nanomos are nearly identical in the +ve gate voltage range in which the vertical electric field is so strong that the separation of energy levels is large and the electrons almost reside in the first subband, thus, the effects of higher subbands is negligible. Conversely, in the −ve gate voltage

DOI: 10.1002/jnm

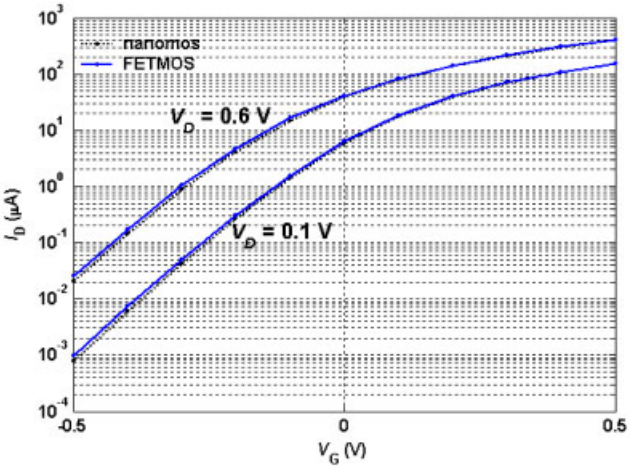

Figure 10. I_D–V_G characteristics at two different values of drain voltage 0.1 and 0.6 V.

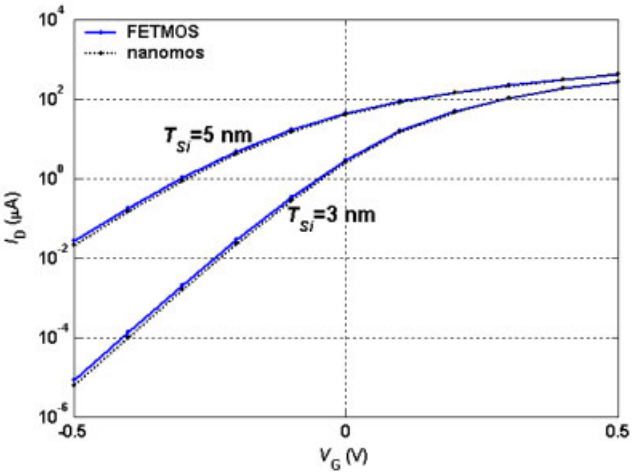

Figure 11. I_D–V_G characteristics at two different silicon film thicknesses 3 and 5 nm, both at $V_D = 0.6$ V.

range, small discrepancy between FETMOSS and nanomos results is due to the effectiveness of higher subbands better accounted by TMM. Another I_D–V_G characteristics found at $V_D = 0.6$ V for $T_{Si} = 3$ and 5 nm is drawn in Figure 11, from which, it is deduced that better subthreshold slope is obtained for smaller thickness devices.

6. CONCLUSION

A device simulator is successfully developed for the simulation of DG SOI n-MOSFETs. The simulator uses finite elements method for the solution of Poisson equation and either of TMM or FDM in the solution of Schrödinger equation. The results of the developed simulator were

DOI: 10.1002/jnm

compared to the quantum device simulator nanomos 2.5 of Purdue University. The use of FEM enables the simulation of curved boundary devices which is not possible by the use of FDM. Furthermore, the use of TMM when higher subbands come into play gives more accurate results than FDM, or equivalently, saves the simulation time. As an example, for an accuracy level of 1%, the use of TMM results in a reduction in simulation time by a factor of nearly 18 times when 10 subbands are taken into consideration.

REFERENCES

1. Fischer C, Habas P, Heinreichsberger O, Kosina H, Lindorfer P, Pichler P, Potzel H, Sala C, Schutz A, Selberherr S, Stiftinger M, Thurner M. *Minimos 6 User's Guide*. Institut fur Mikroelktronik, Technidche Universitat: Wien, 1994.
2. Beebe S, Rotella F, Sahul Z, Yergeau D, McKenna G, So L, Yu Z, Wu K, Kan E, McVittie J, Dutton R. Next generation Stanford TCAD-PICES 2ET and SUPREM 007. International Electron Devices Meeting, San Francisco, 1994; 213–216.
3. Technology Modeling Associates Inc. *TMA medici*, *Two-dimensional Device Simulation Program*, Version 4.0 user's manual. Sunnyvale, CA, 1997.
4. ISE Integrated System Engineering AG. *DESSIS-ISE*, *ISE TCAD release 6.0*. Zurich, Switzerland, 1999.
5. Vasileska D. Self-consistent 1D Schrodinger–Poisson solver. Arizona State University, http://punch.ecn.purdue.edu/Member/CeHub/Program/Schred/
6. The Nanotechnology Simulation Hub. Online computing for nanotechnology, http://nanohub.purdue.edu/NanoHub/
7. Ottosen N, Petterson H. *Introduction to the Finite Element Method*. Prentice-Hall: New York, 1992.
8. Venugopal R, Ren Z, Datta S, Lundstrom MS. Simulating quantum transport in nanoscale MOSFETs: real versus mode space approaches. *Journal of Applied Physics* 2002; **92**:3730–3739.
9. Snowden CM. *Semiconductor Device Modelling*. Peter Peregrinus: London, 1988.
10. Abdolkader TM, Hassan HH, Fikry W, Omar OA. Solution of Schrödinger equation in double-gate MOSFETs using transfer matrix method. *Electronic Letters* 2004; **40**(20):1307–1308.
11. Rahman A, Guo J, Datta S, Lundstrom MS. Theory of ballistic transistors. *IEEE Transactions on Electron Devices* 2003; **50**(9):1853–1864.
12. Ren Z, Venugopal R, Goasguen S, Datta S, Lundstrom MS. NanoMOS 2.5: a two-dimensional simulator for quantum transport in double-gate MOSFETs. *IEEE Transactions on Electron Devices* 2003; **50**:1914–1925.
13. Blakemore JS. Approximation of Fermi–Dirac integrals especially the functions $F_{1/2}(\eta)$ to describe electron density in a semiconductor. *Solid-State Electronics* 1982; **25**:1067–1076.
14. Ren Z. Nanoscale MOSFETs: physics, simulation, and design. *Ph.D. Dissertation*, Purdue University, West Lafatette, IN, October 2001.
15. Kalotas TM, Lee AR. The bound states of a segmented potential. *American Journal of Physics* 1991; **59**(11): 1036–1038.
16. http://www.mathorks.com
17. Shewchuk JR. Delaunay refinement mesh generation. *Ph.D. Dissertation*, Camegie Mellon University, Pittsburgh, May 1997.
18. Rose DJ, Bank RE. Global approximate Newton methods. In *Numerische Mathematik*, Springer: Berlin, Germany, 1981; 279–295.

AUTHORS' BIOGRAPHIES

Tarek M. Abdolkader was born in Cairo, Egypt in 1970. He received BS degree in Electrical Engineering (Electronics and Communications) from the Faculty of Engineering, Ain Shams University, Cairo in 1992, another BS degree in Physics from the Faculty of Science, Ain Shams university, Cairo in 1996, MS and PhD degrees in Engineering Physics from the Faculty of Engineering, Ain Shams university, Cairo in 2001 and 2005, respectively. He is currently an assistant professor of Engineering Physics at the Department of Basic Sciences, Benha Higher institute of Technology, Benha, Egypt. His research interests are modelling of quantum-mechanical effects and development of simulation tools for modern electronic devices, especially, double-gate SOI MOSFETs.

DOI: 10.1002/jnm

Wael Fikry Farouk was born in Cairo, Egypt in 1962. He received the BS degree in Electrical Engineering from Ain Shams University, Faculty of Engineering, Cairo, Egypt in 1984 and the MS and PhD degrees in Engineering Physics from the same university in 1989 and 1994, respectively. He is currently associate professor of Solid-State Electronics in the Engineering Physics Department. His research interests include VLSI MOSFET and SOI devices characterization and modelling, solar cells and silicon-electrochemical cells.

Omar Abdelhalim Omar received the BSc in special Physics from Ain Shams University, Cairo, Egypt in 1963. He received the PhD in Solid State Physics from Electrical Engineering University, Leningrad, Russia in 1970. He joined the Engineering Physics Department, Faculty of Engineering, Ain Shams University in 1971 as an assistant professor. In 1981, he became a professor of Engineering Physics in the same department. His research interests include optical and photoelectrical properties of semiconductors and characterization of solid-state devices.

Mahmoud Fathy Mahmoud Hassan was born in 1948, Egypt. He received his MSc in Quantum Electronics in 1980 and PhD in Physics in 1982 from Essex University, U.K. He joined Benha Institute of Technology as an Associate Professor in 1997. He is a Visiting Professor in National Institute of Laser Enhanced Sciences, Cairo University since 1996 up till now. His research interest is in semiconductor devices, solar cells and interaction of laser with semiconductor.

DOI: 10.1002/jnm